

## Original Article

# Establishment of C6 brain glioma models through stereotactic technique for laser interstitial thermotherapy research

Jian Shi, Ying Zhang<sup>1</sup>, Wei-ming Fu, Minjiang Chen<sup>2</sup>, Zheng QiuDepartments of Neurosurgery, <sup>1</sup>Neuroscience Care Unit, Jiande Branch Hospital, <sup>2</sup>nd Affiliated Hospital, School of Medicine, Zhejiang University, Hangzhou 310009, <sup>2</sup>Neurosurgery, Taizhou First People's Hospital, Zhejiang 318200, ChinaE-mail: Jian Shi - [shishi74@163.com](mailto:shishi74@163.com); Ying Zhang - [daqingzy1978@163.com](mailto:daqingzy1978@163.com); Wei-ming Fu - [Fwm195921@hotmail.com](mailto:Fwm195921@hotmail.com); \*Minjiang Chen - [rivercmj@gmail.com](mailto:rivercmj@gmail.com); Zheng Qiu - [249327830@QQ.com](mailto:249327830@QQ.com)

\*Corresponding author

Received: 24 March 14 Accepted: 12 January 15 Published: 01 April 15

**This article may be cited as:**Shi J, Zhang Y, Fu Wm, Chen M, Qiu Z. Establishment of C6 brain glioma models through stereotactic technique for laser interstitial thermotherapy research. *Surg Neurol Int* 2015;6:51. Available FREE in open access from: <http://www.surgicalneurologyint.com/text.asp?2015/6/1/51/154451>

Copyright: © 2015 Shi J. This is an open-access article distributed under the terms of the Creative Commons Attribution License, which permits unrestricted use, distribution, and reproduction in any medium, provided the original author and source are credited.

## Abstract

**Objective:** To establish C6 brain glioma models using stereotactic technique, and to study effects of laser interstitial thermotherapy (LITT) in rat models of glioma.**Methods:** C6 glioma cells were cultured in dulbecco's minimum essential medium (DMEM) cell culture medium. The *in vitro* C6 cell cultures were stereotactically implanted into the right caudate nucleus of rat brain. Presence of tumor was confirmed with Factor VIII R, hematoxylin–eosin stain, staining of glial fibrillary acid protein, and S-100 immunohistochemistry. After magnetic resonance (MR) scanning and correction of tumor location, the models were divided into groups according to the treating time and laser power (2–10 W). Semiconductor laser optical fibers were inserted in tumors for LITT. Cortex's temperature conducted from the center target was measured using infrared thermograph, and deep-tissue temperature around the target was measured using a thermocouple.**Results:** Rat C6 gliomas were inoculated with optimized stereotactic technique. These gliomas resembled human glioma in terms of histopathological features. Such models are more reliable and reproducible, with 100% yield of intracranial tumor and no extracranial growth extension. The difference between cortex temperature conducted from center target and deep-tissue temperature around target was not statistically significant.**Conclusion:** The rat C6 brain glioma model established in the study was a perfect model to study LITT of glioma. Infrared thermograph technique measured temperature conveniently and effectively. The technique is noninvasive, and the obtained data could be further processed using software used in LITT research. To measure deep-tissue temperature, combining thermocouple with infrared thermograph technique would present better results.**Key Words:** Glioma, laser, rat models, thermotherapy**Access this article online****Website:**[www.surgicalneurologyint.com](http://www.surgicalneurologyint.com)**DOI:**

10.4103/2152-7806.154451

**Quick Response Code:**

## INTRODUCTION

Laser interstitial thermal therapy (laser interstitial thermotherapy, LITT) is a kind of minimally invasive

neurosurgery treatment strategy that is increasingly being used in clinical practices. The therapy is characterized by good orientation, energy concentration, and ease of control, but the temperature measuring technology

remains to be improved.<sup>[3,10,15]</sup> For rat glioma model, there is extensive literature available, while only a few reports from animal models are available for LITT treatment of intracranial glioma.<sup>[5,12,19]</sup> In the present study, a rat stereotactic apparatus (Jiangwan II) was used to study LITT. In this process, C6 glioma cells were implanted into the right caudate nucleus area of Sprague-Dawley (SD) rats, excluding the extracranial channel. Semiconductor laser optical fiber was imported for the experiment, and magnetic resonance imaging (MRI) was used to assess tumor cell growth after implantation. In addition, application of LITT was investigated under varying conditions, and temperatures measured using a thermocouple and by infrared thermal imaging were compared.

## MATERIALS AND METHODS

### Experimental animals, cells, and reagents

A total of 60 male SD rats (body weight 210–250 g; mean 230 g) were purchased.

The C6 glioma cells were purchased from the Chinese Academy of Sciences, Shanghai Institute of Cell Biology (Shanghai, China). Factor (F) VIII R, glial fibrillary acidic protein (GFAP), and S-100 protein antibody I were bought from Sigma Company.

The following instruments and systems were also used: Immunohistochemical detection kit (Boster company, China); rat stereotactic apparatus (Jiangwan II); 4.7 T BIOSPEC30 type magnetic resonance tomography (Wuhan Institute of Physics and Mathematics of the Chinese Academy of Sciences); and DIOMED60 type semiconductor laser diode (DIOMED company). The advanced fourth-generation aluminum gallium arsenic diode laser had a wavelength range of 790–830 nm and adjustable power output of 0.5–60 W. ThermaCAM S65 type infrared thermal image thermometer and thermocouple thermometer, both manufactured by Raytek company, were used for temperature measurement.

### Stereotactic inoculation treatment

The C6 glioma cells were cultured in DMEM cell culture medium containing 10% fetal bovine serum in an incubator containing 5% CO<sub>2</sub> at 37°C. In logarithmic growth phase of cells, the cell concentration for every 10 µl of cell suspension was 1 × 10<sup>6</sup> C6 cells (temperature table at 37°C). When the cells reached the log phase, they were set aside for further use. Animals were anesthetized and randomly immobilized on the Jiangwan II stereotactic apparatus, according to the big mouse stereotactic map point—on the right side of the caudate nucleus as 1 mm front coronal suture, 3 mm on the right side to central, and 5 mm deep.<sup>[2]</sup> The stereotactic apparatus uses a set of three coordinates (X, Y, and Z). The point of

craniotomy was determined by adjusting X, Y axis knobs. Incisions were made on the skull in quincunx-shaped foraminula with spherical micro-drilling, and the holes were expanded up to Ø 2.5 mm. The thin layers of the dura mater could be found through the foraminula. Each extracted 20 µl C6 cell suspension in trace syringe was fixed at 90 degrees, Z-axis knob was adjusted and the needle was vertically inserted up to 6 mm, with 1 mm return. The cell suspension was injected into the caudate nucleus at the rate of 4 µl/min. After the injection, the needle should be kept inserted for 2–3 min, and should be pulled out slowly after 2 min. Finally, a sterile polyvinyl chloride (PVC) tube was merged, the diameter of the tube was 2 mm and the length was 3 mm. The skull was closed with zinc phosphate around the tube and the internal tube was temporarily sealed off with a small amount of bone wax [Figure 1].

### MRI monitoring and histopathology

For enhanced MRI scanning, gadolinium diethylenetriaminepentaacetic acid (GD-DTPA; contrast medium) was injected into the SD tumor-burdened rats, peritoneally (5 ml/kg) on the 5<sup>th</sup>, 10<sup>th</sup>, 15<sup>th</sup>, and 20<sup>th</sup> day after stereotactic experiment. After the last MRI scanning, the C6 glioma rats were sacrificed by cerebral perfusion fixation and 2 mm coronary brain sections were taken. Gross pathological research was performed on these sections. The factor VIII-related antigen (FVIIIIRAg), GFAP, and S-100 protein expression were analyzed in C6 glioma, according to the immunohistochemical method. The tumor microvascular counts (MVDs) were calculated using FVIIIIRAg as the marker for tumor vascular endothelial cells. The concentration of primary antibody VEGF, S-100, and FVIIIIRAg was 1:100, 1:200, and 1:200, respectively.

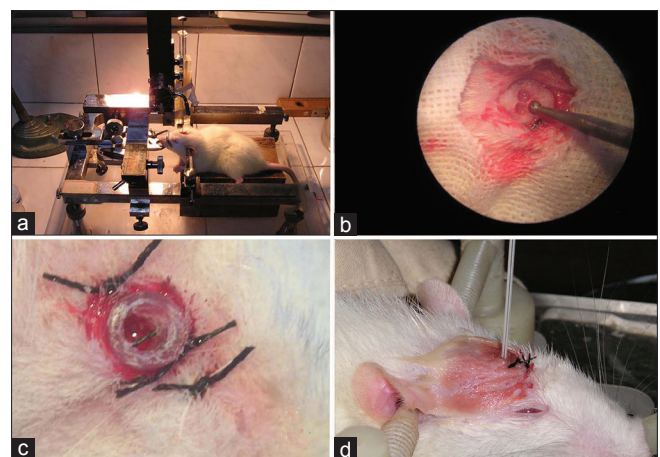


**Figure 1: Stereotactic inoculation of C6 cells (a) Rats were fixed in the stereotaxic apparatus and micropipette tip was positioned. (b) In accordance with the stereotaxic atlas, the transcranial point was adjusted, a "A" shaped skull hole was made with a dental spherical drill under a microscope. (c) A sterile PVC tube was fixed on the scalp as a treatment channel. Bone wax was used to seal it. (d) LITT test: Insertion of laser fiber**

## LITT experiment and infrared temperature measurement applications

A total of 16 experimental rats were randomly divided into three thermal groups (A, B, C) on the 20<sup>th</sup> day. Rats in Group A were subjected to laser treatment of 2 W with 900 s of thermal action time, and the temperature was measured using infrared thermal imaging technique. Rats in Group B were subjected to laser treatment of 10 W with 400 s of thermal action time. The temperature was measured using a thermocouple. In Group C, the output laser power was available from 2 to 5 W with a thermal action time of 600 s. In this group, the infrared thermal imaging and thermocouple temperature measurement were applied simultaneously. Furthermore, 10 experimental rats were randomly assigned to form Group D (control group). In the control group, the laser fibers were inserted without any output power, and temperature was measured using both methods. In thermal groups, postanesthesia care, the rat heads were fixed on stereotactic apparatus, then semiconductor laser fiber tubes were inserted to pass through the PVC tube and skull hole. The insertion direction was adjusted to ensure fiber tip focus on the glioma center, according to previous MRIs. New adjustments could be made in terms of laser power or action time accordingly. The laboratory environment was maintained without any disturbance at a constant temperature of 22°C and humidity of 50%. Heat was conducted for 90 s and then measurement of temperature was started. In Group A or C, a ThermoCAM S65 infrared thermal imager was hung on top of the rats at a distance of 0.5 m for real-time values, and the focal length was adjusted to measure the cortex conduction temperature from center targets. In Group B or C, a thermocouple godet was slowly inserted near the thermal target at a distance of about 4 mm, to achieve single-point temperature around deep glioma. The specifications of postoperative treatment were as follows: PVC tube should be sealed using sterile bone wax, and 8 ml cool saline should be injected intraperitoneally. The thermographic figure could be analyzed in assistance with ThermoCAM QuickView software, which could draw the maximum temperature, minimum temperature, average temperature, and arbitrary point temperature in the thermal therapy target area [Figure 2].

### Statistical analysis

The variables of MRI measurements and temperature were represented as ( $\bar{x} \pm s$ ) mm and ( $\bar{x} \pm s$ )°C. SPSS 11.0 statistical software was used for the *t*-test and *P* < 0.05 were considered statistically significant.

## RESULTS

### Signs of glioma growth

*In vivo* experiment showed that the tumor formation rate was 96.67% in the rats from the point of inoculation with

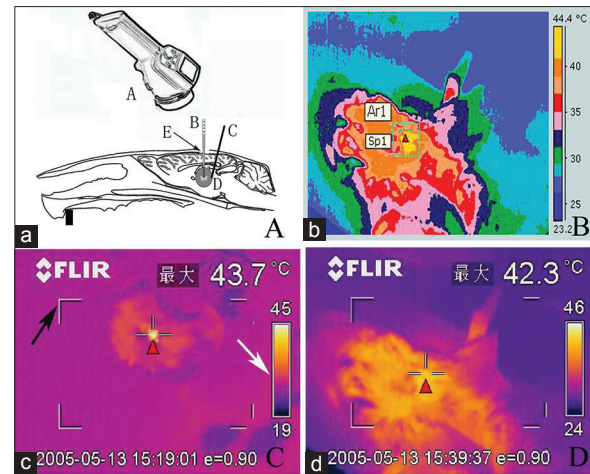


**Figure 2: Experimental rat LITT treatment (a) ThermoCAM S65 type infrared thermometer (A), opened skull window of rat (E). The laser fiber (B) rat brain glioma entity (D), thermocouple electrodes (c) inserted at glioma edge. (b) Image of infrared temperature measurement instrument records. (c) The highest temperature of corresponding regions is displayed, black arrow indicating the viewfinder and white arrow indicating thermal imaging color levels. (d) The target temperature is real-time, as detected on thermal infrared imager, displaying cortex temperature on center target. (Red triangle)**

C6 glioma cell suspension to the point of death. In the initial 2 days, experimental rats gradually restored diet and activities, followed by evident weight loss by 7–15 days. By 11–15 days, depression in performance was observed along with docile behavior and decreased activity. By 10–20 days, the animals presented instability in walking, hemiplegia, and intermittent seizures. All these symptoms aggravated by 15–20 days along with presence of anorexia-cachexia, eye conjunctival congestion on the right side or double sides or increased seizure frequency. After 20 days, the rats showed limbs buckling, twitch, and severe weight loss. Experimental rat survival times were as follows: Group A 47.00 ± 4.11 days; Group B 42.00 ± 3.12 days; Group C 51.00 ± 7.13 days; and Group D 34.00 ± 3.91 days.

### MRI dynamic scanning

Five-day postcommencement of the experiment, 58 tumor-burdened rats displayed lesions on the MRI. Ten days postinoculation, the growth of C6 gliomas were visible on the right caudate nucleus, which was shown as equisignal or slightly low signal intensity on T1-weighted images (T1WI) and high signal intensity on T2-weighted images (T2WI). The surrounding tissue boundary was clear, and the diameters of the tumors ranged 2–4 mm. Tumors increased gradually until 15 or 20 days of inoculation, and the evident mass effect with clear boundary could be seen as oval or irregular shape; the diameter of the tumors reached 5–8 mm. On T2WI the edematous surrounding tissues and mass effect were demonstrated more apparently. In addition, contrast enhanced T1WI scanning clearly improved the images of the masses and the boundaries [Figure 3].

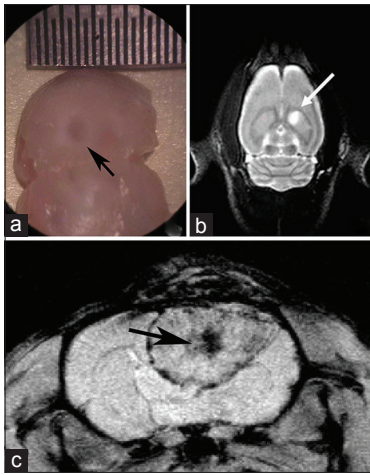


**Figure 3:** C6 rat brain glioma MRI detection (a) C6 cell suspensions were inoculated. After 5 days of inoculation, a tumor of diameter 3 mm was seen under the microscope. (b) On T2 MRI, a high-signal intensity lesion was found on the right caudate nucleus. (c) Twenty days after inoculation, the tumor was visible on axial T1 MRI scanning, and the demarcation of the intra-brain glioma mass was clear with a central necrosis

### Comparison of LITT temperature measurement methods

Temperature was measured in the three groups (A, B, C) for a duration of 300 s of thermal therapy. The measured temperature was calculated as  $\bar{x} \pm s^{\circ}\text{C}$ . In Group A, the temperature was measured by infrared thermal imaging. According to intraoperative real-time thermal images shown on an liquid-crystal display (LCD) screen, variation in temperature could be observed from center targets to cortex images. The average maximum temperature was recorded as  $(41.9 \pm 2.2)^{\circ}\text{C}$ . In Group B, the surrounding tissues were located at a distance of 2 mm from the laser fiber tip by inserted thermocouple stromal tumors, and thermal conducted temperatures were measured as  $(42.4 \pm 1.8)^{\circ}\text{C}$ . In Group C, laser fiber and thermocouple godet were inserted, and real-time output power was adjusted between 2 and 5 W. Based on the readings shown on the thermal imager screen, the highest temperature conducted from center targets to cortex was ensured above  $42^{\circ}\text{C}$ , and the average was  $(42.5 \pm 1.4)^{\circ}\text{C}$ . The average temperature of surrounding tissue was measured as  $(42.1 \pm 1.9)^{\circ}\text{C}$ . Group D was treated as the control group, where the cortex temperature was  $(36.5 \pm 0.9)^{\circ}\text{C}$  and the tumor interstitial tissue temperature was  $(37.2 \pm 0.5)^{\circ}\text{C}$ . On comparing the thermal therapy groups (Groups A and B) with Group D, it was found that the temperature differences were statistically significant ( $P < 0.05$  and  $P = 0.021$ , respectively). In Group C, when the cortex highest temperature conducted from center target and the interstitial temperature surrounding the tumor were compared, it was found that there was no statistically significant difference ( $P > 0.05$ ,  $P = 0.05$ , respectively) [Figure 4].

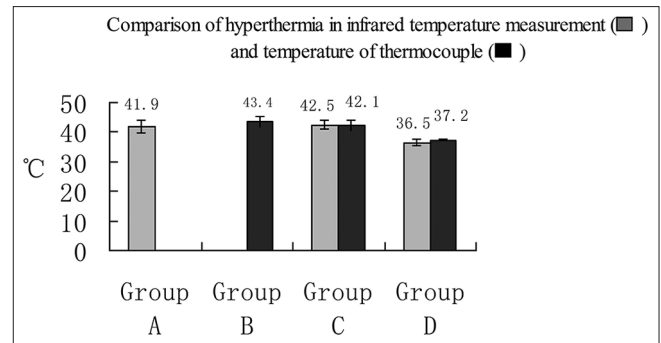


**Figure 4:** Comparison of two methods of measuring temperature. Temperature measurement was carried out in the three groups (A, B, C) in a period of 300 s of thermal therapy. Group D was the control group. In Group C, no statistically significant difference was found between the cortex highest temperature conducted from center target and the interstitial temperature surrounding the tumor

### Pathology observation

Research of macropathology demonstrated that malignant glioma occupy most of the right hemisphere and extended into the contralateral hemisphere from the corpus callosum. Post-HE dyeing, the tumors were composed of false capsular, C6 glioma mass, and central ischemic necrosis area with closed morphological characteristics of human malignant glioma. Immunohistochemical analysis showed that in the cytoplasm, GFAP, and S-100 protein were positively expressed. In addition, the tumor microvasculars were proliferated significantly, which was confirmed by positive expression of FVIIIIRA [Figure 5]. The LITT treatment group showed differential tissue damage. In Groups A and C the noncarbide coagulation and necrosis edema area were generated, whereas in Group B carbide, thermal condensation, and necrosis edema area were produced.

### DISCUSSION

Rat intracranial glioma models have some advantages over the nude mice subcutaneous heterogeneous glioma models. The advantages are as follows: The growth characteristics resemble the characteristics of human malignant glioma; these models are easy to raise and are of lower cost; they accept all *in vivo* experiments including immunotherapy and high-simulating brain tissue environment. At present, the applicable rat glioma cell lines involve C6, 9 l, T9, F98, RG2 (D74), BT4C, and CNS-1. The C6 glioma models produced by inoculation of standard quantitative C6 brain cells into the rat brain with stereotactic technique were the earliest as well as most widely and commonly applied models.<sup>[2,11,19]</sup> With continuously improving inoculation technology, to explore inoculation repeatability, Morreale<sup>[12]</sup> had inserted stainless steel tubes into rat caudate nucleus. Although inoculation channel could be realized through these methods, they posed several disadvantages. For example,

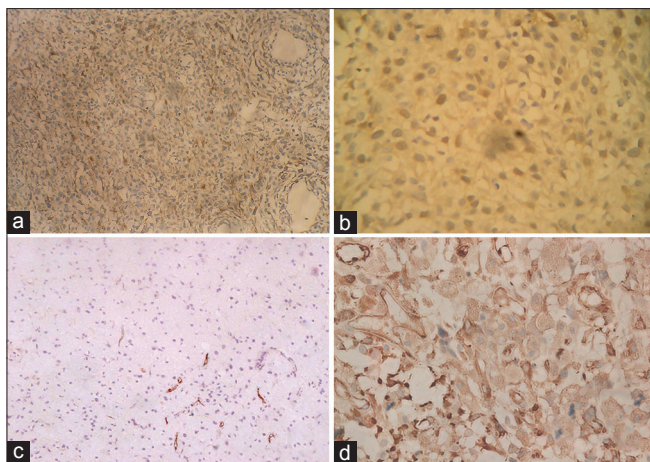


**Figure 5: Histopathology of rat C6 glioma model (a) Astrocytoma showed (two staining  $\times 100$ ). (b) The brown staining was found in the cytoplasm, S-100 protein was positively expressed in the immunohistochemical staining ( $\times 200$ ). (c) FVIIIIR was positive and microvessel hyperplasia is shown ( $\times 200$ ). (d) On the background of C6 astrocytoma, the brown stain illustrates GFAP positive expression ( $\times 200$ )**

the materials used were unique and involved high cost; surgical procedures were complex or inconvenient; and there was an increase in brain damage of varying degree, which could change the growth of glioma in natural state. In the present study, we had implanted permanent PVC pipe and buried extracranial tip under the scalp. Currently, nude mice or rat glioma subcutaneous transplantation tumor models are used as animal models to study thermal therapy. Rat intracranial glioma models applied to interstitial thermal therapy that can perform real-time monitoring of temperature change have been reported rarely.<sup>[5,6,16,18,19]</sup>

In the present experiment, some adjustments were made according to the actual needs: (i) If C6 cell suspension system was accomplished, compared with putting it in a constant-temperature bath box at 37°C using a thermostatic shaker, precipitation or squeezing of the suspension could be avoided to keep the stability in certain concentration to ensure that the suspension is preserved for a longer duration. (ii) One key point was “enter 6 back 1” after puncture to leave 1 mm gap at front tip, injecting cell suspension for 2 min, and holding the needle for 2–3 min. C6 cells could be sedimented and spread out fully. Another key point was that the needle should be pulled out slowly (at least 2 min), especially in the starting stage, to prevent the siphoning effect. Otherwise, this siphon effect could bring the suspension into the puncture tunnel and cause potential extracranial metastases. (iii) Since the rat skull is thin, microsurgery becomes necessary for making or extending bone window to 3 mm in diameter. We designed an extracranial PVC pipe and placed it for further treatment and used it as a drug delivery channel. (iv) When GD-DTPA was injected into the rat tail vein,

it becomes difficult to conduct the method on a routine basis.<sup>[4,6,17]</sup> So, in our experiment, GD-DTPA (5 ml/kg) was injected peritoneally in the experimental rats, which made the method convenient and repeatable. After the above improvisations, the success rate of transplanted glioma was higher without extracranial metastases. The PVC channels were convenient and easy to operate, and caused no further brain damage. After 3–5 days of inoculation, the implanted tumor could be confirmed by MRI, macropathology, or pathologic histology, which would extend its volume increase oppression and high cranial pressure symptoms gradually along with time. The fastest tumor growing period was between 2 and 3 weeks, and then the speed of growth slowed down dramatically. According to the tumor growth characteristics of the model, it is generally believed that the advisable time of experiment treatment were between 5 and 10 days,<sup>[6,11,16,19]</sup> during which the interstitial thermotherapy, chemotherapy, drug intervention, or immunotherapy could be completed. In the present experiment, we confirmed that capillary hyperplasia and the blood–brain barrier structure was present in rat glioma models, which presented high similarity with human glioma in terms of histopathological characteristics. MRI scanning was sensitive and effective for evaluating tumor growth. Although the tumor progression of experimental rats had certain regularity in general, some individual differences existed. As a living dynamic monitoring method, MRI provides visual images that contribute to correction of stereotactic direction of the laser fiber during LITT treatment. While considering factors such as high cranial pressure and cerebral edema, cerebral malignant tumors are contraindications to whole body heat. It was relatively safe and effective that implanted electrodes microwave antenna, or thermal seeds were used to realize interstitial heating brain by stereotactic technique.

In recent years, LITT technology is increasingly being used in laser medicine. This technology transformed photon energy into thermal energy through inserting the laser fiber into the organization and introducing a kind of laser at a specific wavelength. The related tissue was heated gradually, which caused short-term thermal effect such as cutting, gasification, and carbonized solidification. In addition, by adjusting to a certain wavelength, power, pulse width, and intermittent pulse mode to realize the compensation to heat fading, antitumor effect was achieved, which originated from effective thermal therapy temperature and heat distribution.<sup>[3,10,15]</sup> In our anterior research, we supposed the 4 mm distance away from the LITT target, which could be considered as surrounding tissue. Monitoring of real-time temperature using a measuring system is very important during thermal therapy. Some researchers commented: “No temperature measurement, no thermal therapy”.<sup>[10]</sup> Other than the widely used invasive thermocouple thermometer, thermal

resistance thermometer, and optical fiber thermometer, some studies have used ultrasound, MR thermal image, and infrared thermal image techniques, to achieve the noninvasive temperature measurement.<sup>[1,6,7,14,18,19]</sup>

Infrared thermal image map is a two-dimensional colorful temperature distribution field. We consider it as a kind of surface temperature measurement technology that measures temperature at the point of scalp or skull. However, this method cannot represent the deep brain temperature due to the presence of the skull. In our experiment, the bone windows of more than 3 mm diameter were created, which minimized the skull or skin barrier, due to which the surface temperature could be considered similar to the experimental tumor tissue temperature of rats that were not located very deep. While comparing the two methods of measuring temperature at the same power and action time in Group C, we illustrated an assumption that the cerebral cortex temperature conducted from LITT target could be recorded by infrared temperature measuring system. It could be approximated with the tumor surrounding temperature, which was also conducted from thermal therapy target [Figure 2]. During the present LITT experiment, the thermal energy from targets presented attenuating transmission, which occurred symmetrically in the interstitial tissue of substantial mass. On the infrared thermal image, the temperature of the cerebral cortex was shown directly, which could be treated as the tumor surrounding temperature rather than the target temperature. Clinical hyperthermia chemotherapy research could be practiced at the same time, while conducting craniotomy to remove tumors. On the one hand, surgery exposed the tumors by removing the barriers of the skull or skin. On the other hand, the infrared temperature measurement technology provided the possibility of noninvasive and contactless real-time temperature measurement technique.

The advantages of infrared thermal imaging temperature measurement technology included quick and simple operation, sufficient measurement area, sterile contactless style, noninterference to surface temperature field, storable real-time thermal image, and further software analysis.<sup>[8,13]</sup> Another advantage of this measurement technology was monitoring of the temperature of tumor area as well as monitoring of the temperature of experimental animals.<sup>[3]</sup> However, this technology was a kind of surface temperature measurement technique, in which the temperature of deep tissues could not be measured directly. In addition, the accuracy of this technique was affected by the emissivity or density of the experimental object or the environmental temperature. A certain degree of measurement error also existed. To overcome these disadvantages it was combined with thermocouple interstitial temperature measuring method. Both the methods in combination could be reduced as

“dot + surface” type method, which could maximize strengths and minimize or circumvent weaknesses.

The effective antitumor temperature of LITT was usually considered as 41–45°C. In our research, according to the distance from the thermal therapy target, the temperature showed a sharp drop. The key technology of LITT treatment should maintain a safe and stable temperature in the target tissue region. Generally it was approved that the acting temperature at the tumor periphery should reach 41–43°C, the temperature range at which malignant tumor cells showed a much higher sensitivity to heat injury than normal tissues.<sup>[8]</sup> While temperature is affected by various factors such as heating method, action time, heat power, and varying tissue density, in our study, we used the semiconductor laser system. In Group C, the adjusted output was of a wavelength of around 1060 nm, power 2–5 W, and acting time 600 s. In this group, monitoring was done through infrared thermometer and thermocouple temperature measurement instrument. Output power was increased gradually and was adjustable. Experimental rats showed antitumor effect but survived safely and presented good tolerance. Hence the tumor surrounding temperature was controlled at about 42°C. In addition, a single-time LITT treatment was practiced for rat intracranial glioma model in which the diameter was 3–5 mm. The temperature distribution and thermal condensation covering zone were satisfactory. The high output power of laser produces significant heating and gasification, gasification pressure, and gas flow counter punching. All these factors aggravate brain injury and may also bring about cerebral hemorrhage, cerebral edema, and increased intracranial pressure. It was found that, prolonged time and small power output were unable to raise the instantaneous firing temperature or gas expansion. In this way, we could obtain enough noncarbonization heat condensation damage range at the target tissue, and at the same time, we were able to reduce the heat damage or edema to the surrounding brain tissue with more safety. Based on the photon transport theory, some studies used mathematical simulation method and bio-heat transfer equation in biological tissue energy distribution and temperature distribution.<sup>[14,18]</sup> Emily<sup>[5]</sup> reported an experiment in which near-infrared-absorbing silica-gold nanoshells were injected in murine glioma models and the models were exposed to a near-infrared laser. The experiment showed a significant improvement in survival of the experimental animals. Except LITT, nanoshell-mediated laser photothermal therapy represents a promising novel treatment strategy for malignant glioma. Thermal analysis assisted with MR temperature mapping in the rat glioma model during hyperthermia that incorporated magnetic nanoparticles (MNPs) was real-time and noninvasive, but required nonmagnetic therapeutic environment,<sup>[9,11]</sup> which makes it impractical in LITT.

This experiment provides a successful rat intracranial glioma model and preliminary noninvasive infrared temperature measurement technology for the study of brain glioma stereotactic LITT treatment. In contrast to human brain, the rat glioma tumor was much smaller, due to which stereotactic localization became relatively simple. Although the present LITT experiments were single-time therapy, if necessary, we can realize multiple intracranial LITT treatments through extracranial PVC tubes. With the developments of multi-subject technology, clinical LITT operation assisted with imaging technique and stereotactic fractionated dose multi-treatment technology can be prospected. The noninvasive multi-point temperature measurement and software technology will certainly continue to develop.

## REFERENCES

1. Arthur RM, Straube WL, Trobaugh JW, Moros EG. Non-invasive estimation of hyperthermia temperatures with ultrasound. *Int J Hyperthermia* 2005;21:589-600.
2. Barth RF, Kaur B. Rat brain tumor models in experimental neuro-oncology: The C6, 9L, T9, RG2, F98, BT4C, RT-2 and CNS-1 gliomas. *J Neurooncol* 2009;94:299-312.
3. Carpentier A, Chauvet D, Reina V, Beccaria K, Leclercq D, McNichols RJ, et al. MR-Guided Laser-Induced Thermal Therapy (LITT) for Recurrent Glioblastomas. *Lasers Surg Med* 2012;44:361-8.
4. Cha S, Johnson G, Wadghiri YZ, Jin O, Babb J, Zagzag D, et al. Dynamic, contrast-enhanced perfusion MRI in mouse glioma: Correlation with histopathology. *Magn Reson Med* 2003;49:848-55.
5. Day ES, Thompson PA, Zhang L, Lewinski NA, Ahmed N, Drezek RA, et al. Nanoshell-mediated photothermal therapy improves survival in a murine glioma model. *J Neurooncol* 2011;104:55-63.
6. eL-Ouahabi A, Guttman CR, Hushek SG, Bleier AR, Dashner K, Dikkes P, et al. MRI guided interstitial laser therapy in a rat malignant glioma model. *Lasers Surg Med* 1993;13:503-10.
7. Gellermann J, Włodarczyk W, Ganter H, Nadobny J, Föhling H, Seebass M, et al. A practical approach to thermography in a hyperthermia/magnetic resonance hybrid system: Validation in a heterogeneous phantom. *Int J Radiat Oncol Biol Phys* 2005;61:267-77.
8. Gorbach AM, Heiss JD, Kopylev L, Oldfield EH. Intraoperative infrared imaging of brain tumors. *J Neurosurg* 2004;101:960-9.
9. Kickhefel A, Roland J, Weiss C, Schick F. Accuracy of real-time MR temperature mapping in the brain: A comparison of fast sequences. *Phys Med* 2010;26:192-201.
10. Leonardi MA, Lumenta CB, Gumprecht HK, von Einsiedel GH, Wilhelm T. Stereotactic guided laser-induced interstitial thermotherapy (SLITT) in gliomas with intraoperative morphologic monitoring in an open MR-unit. *Minim Invasive Neurosurg* 2001;44:37-42.
11. Liu L, Ni F, Zhang J, Wang C, Lu X, Guo Z, et al. Thermal analysis in the rat glioma model during directly multipoint injection hyperthermia incorporating magnetic nanoparticles. *J Nanosci Nanotechnol* 2011;11:10333-8.
12. Morreale VM, Herman BH, Der-Minassian V, Palkovits M, Klubes P, Perry D, et al. A brain-tumor model utilizing stereotactic implantation of a permanent cannula. *J Neurosurg* 1993;78:959-65.
13. Okudera H, Kobayashi S, Toriyama T. Intraoperative regional and functional thermography during resection of cerebral arterio-venous malformation. *Neurosurgery* 1994;34:1065-7.
14. Schwarzmaier HJ, Eickmeyer F, von Tempelhoff W, Fiedler VU, Niehoff H, Ulrich SD, et al. MR-guided laser-induced interstitial thermotherapy of recurrent glioblastoma multiforme: Preliminary results in 16 patients. *Eur J Radiol* 2006;59:208-15.
15. Sugiyama K, Sakai T, Fujishima I, Ryu H, Uemura K, Yokoyama T. Stereotactic interstitial laser-hyperthermia using Nd-YAG laser. *Stereotact Funct Neurosurg* 1990;54-55:501-5.
16. Tyynela K, Sandmair AM, Turunen M, Vanninen R, Vainio P, Kauppinen R, et al. Adenovirus-mediated herpes simplex virus thymidine kinase gene therapy in BT4C rat glioma model. *Cancer Gene Ther* 2002;9:917-24.
17. Valable S, Barbier EL, Bernaudin M, Roussel S, Segebarth C, Petit E, et al. *In vivo* MRI tracking of exogenous monocytes/macrophages targeting brain tumors in a rat model of glioma. *Neuroimage* 2008;40:973-83.
18. Yung JP, Shetty A, Elliott A, Weinberg JS, McNichols RJ, Gowda A, et al. Quantitative comparison of thermal dose models in normal canine brain. *Med Phys* 2010;37:5313-21.
19. Zhang F, Xie J, Liu G, He Y, Lu G, Chen X. *In Vivo* MRI Tracking of cell invasion and migration in a rat glioma model. *Mol Imaging Biol* 2011;13:695-701.